Table 1. Sequences of PCR Primers

Primer	Sequence (5'-3')	Annealing Temperature (°C)	PCR Product (bp)
GAPDH	CCATCACCATCTTCCAGGAG CCTGCTCACCACCTTCTTG	60	576
Musashi-1	ATGCCATGCTGATGTTCGAC ACCCTGGGTAACCTAACATG	60	255
c-Kit	CATCATGGAAGATGACGAG CAAATGTGTACACGCAGCTG	60	281
Thy1	ACAAGCTCCAATAAAACTATCAATGTGAT GGAAGTGTTTTGAACCAGCAGG	60	84
AFP	TGAAATTTGCCACGAGACGG TGTCATACTGAGCGGCTAAG	60	272
Albumin	GACAAGTTATGCGCCATTCC ACTGGGTCAGAACCTCATTG	60	288
Transferrin	TGTCTGAGCATGAGAACACC GTTCAGCTGGAAGTCTGTTC	60	299
TAT	TACTCAGTTCTGCTGGAGCC GCAAAGTCTCTAGAGAGGCC	60	471
CYP2E1	AGCACAACTCTGAGATATGG ATAGTCACTGTACTTGAACT	60	365
CYP3A1	CAGCTCTCACACTGGAAACCTGGG CTCATATATTTGGGGTGAGGAATGG	60	689
CX43	GGAAAGTACCAAACAGCAGC AGGACTTGTCATAGCAGACG	60	348
CK19	ATGACTTCCTATAGCTATCG CACCTCCAGCTCGCCATTAG	60	340
CX18	GGACCTCAGCAAGATCATGGC CCACGATCTTACGGGTAGTTG	60	515
HNF3α	TTCGGAGTTGAAGTCTCCAG CATATGCCTTGAAGTCCAGC	60	218
HNF4	TCTACAGAGCATTACCTGGC TGAGGGGAAGATGAAGACGG	60	614
C/EBPα	TTCCAGATCGCACACTGCCC TGACCAAGGAGCTCTCAGGC	60	404
HNF6	GACAAATGGCAGGACGAGGG AGCGTACTGGTTTAGGTGCC	60	681

NOTE. GAPDH was used as an internal control.

through 70-μm nylon mesh, and small cell aggregates on the mesh were selectively picked up using a pipette. The cell aggregates were suspended in Dulbecco's modified Eagle's medium supplemented with 10% fetal bovine serum, 10 mmol/L nicotinamide, 1 mmol/L ascorbic acid 2-phosphate, 10 ng/mL epidermal growth factor (Collaborative Research, Lexington, MA), 10^{-7} mol/L dexamethasone, 0.5 μg/mL insulin, and antibiotics. Then 200 cell aggregates were plated on a 35-mm dish. Seven days after plating, the dishes were randomly divided into 3 groups: no treatment (NT), cells overlaid with collagen gel (CG), and cells overlaid with TGP gel (TGP). The specific gravity of both collagen gel and TGP was adjusted to 1.06 mg/mL.

Polymerase Chain Reaction. Total RNA was isolated from ductules and cultured cells, and reverse transcriptase-polymerase chain reaction was conducted as previously described.[10] Primers are listed in Table 1.

Colony Counts. We measured colony number and size using a phase-contrast microscope (Olympus Optical, Tokyo, Japan) equipped with a CCD camera.

Statistics Analysis. Data are shown as mean ± SEM. ANOVA and Fisher's protected least significant difference test were used, and a P value $<.05$ was considered significant.

Results

Histology of the Liver Injury. At day 28, we macroscopically observed complete recovery of liver tissue in the TGP group, whereas in livers of both the control and FG groups fibrosis was apparent in the lesions. As shown in Fig. 1, in the control group, the hole was left open, and exudates accumulated at postoperative day 3 (POD 3, Fig. 1B). Thereafter, inflammatory and fibroblastic cells gradually gathered and formed granulomatous tissue at POD 7, which became larger and more prominent at POD 14 (Fig. 1C) and POD 28 (Fig. 1D). In the FG group, inflammatory cells and fibroblastic cells invaded the FG at POD 3 (Fig. 1F). The FG remained in the center of the lesion and fibrosis was observed at the periphery of the defect at POD 14 (Fig. 1G). Granuloma-

tapraid5/zhe-hepa/zhe-hepa/zhe00506/zhe1258d06g | heckt | S=7 | 3/6/06 | 15:31 | Art: 05-1402

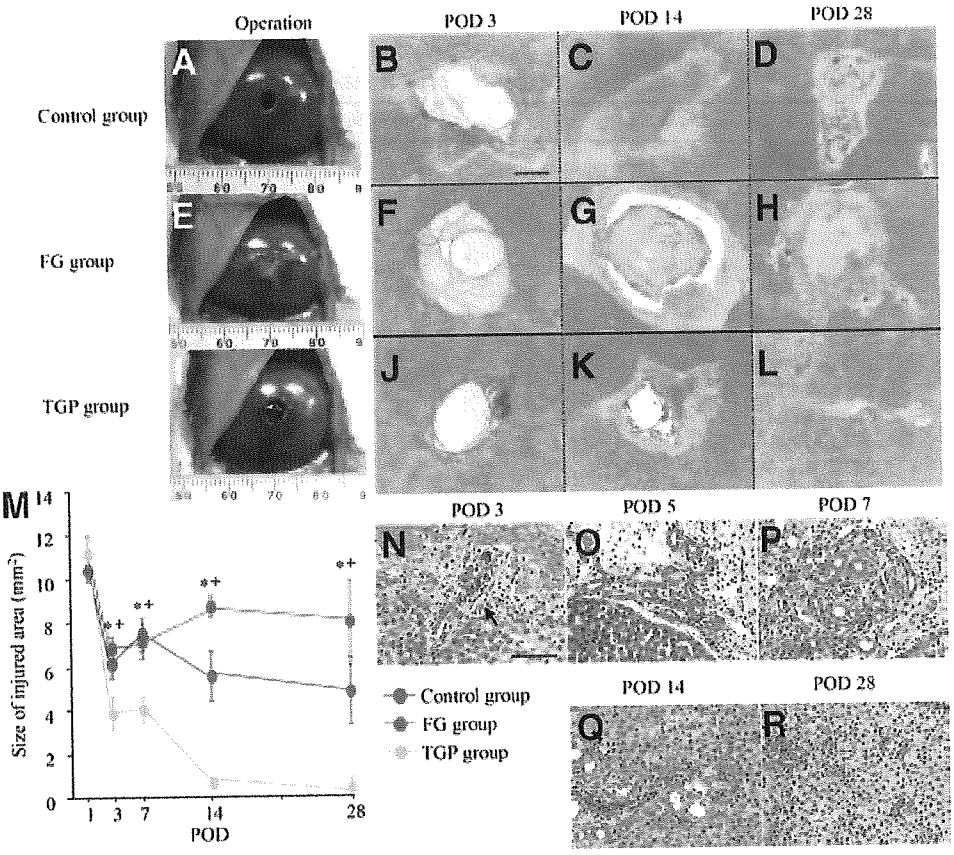

COLOR

Fig. 1. Histological analysis of the partially injured rat liver filled with TGP. A penetrating wound was made in the left middle lobe (A). The hole was left open (control group). Exudates and coagulation accumulated in the injury site at POD 3 (B). Inflammatory cells and fibroblasts gradually formed granulomatous tissue, and scar formation then became evident at POD 14 (C) and POD 28 (D). Fibrin gel was poured into the lesion (E; FG group). The inflammation was evident inside and around the gel at POD 3 (F). FG changed to granuloma and the size of the injured area was enlarged at POD 14 (G). Hepatic regeneration did not occur at POD 28 (H). The hole was filled with TGP (I; TGP group). A thin layer of connective tissues surrounding TGP was observed at POD 3. The area of TGP became small and the injured area gradually shrank at POD 14 (K). Most of the injured area was replaced with hepatic cells, and only a small amount of fibrosis remained at POD 28 (L). B-D, F-H, and J-L show HE staining at the same magnification. Scale bar, 1 mm. Change of the size of the injured area after operation in each group (M). Bars show mean ± SEM of five samples. TGP versus *Control and +FG, $P < .05$. Histological appearance of the liver tissues treated with TGP: Ductular reactions (an arrow) emerged at POD 3 (N). They elongated from the portal areas located at the boundary between intact hepatocytes and dead cells. The ductules extend toward the injured area at POD 5 (O). The cells in ductular reactions became columnar-like structures at POD 7 (P). The hepatocyte-like cells increased around the ductules at POD 14 (Q). On POD 28, most ductules have disappeared and the lesion is almost completely replaced with hepatocytes (R). N-R are the same magnification. Scale bar, 100 μm. TGF, thermoreversible gelation polymer; POD, postoperative day; FG, fibrin glue; HE, hematoxylin-eosin.

tous tissue was observed even at POD 28 and no replacement of hepatocytes was observed (Fig. 1H). In the TGP group, the TGP-occupied area was observed as a vacant area (Fig. 1J) that gradually shrank with time (Figs. 1J-L). Between the vacant area and intact hepatocytes, a relatively narrow area of tissue consisting of epithelial and fibroblastic cells, some inflammatory cells, and fibrosis were observed at POD 14 (Fig. 1K). Although a small amount of fibrosis remained, the lesion was almost completely replaced by hepatocytes at POD 28 (Fig. 1L). As shown in Fig. 1M, the size of the injured area dramatically decreased in the TGP group, whereas it did not change in the FG group and decreased by half in the control group.

To examine whether remnant MHs surrounding the injured area participated the regeneration, we measured the sizes of neighboring lobules. Lobules not only proximal but also distal to the injury were not enlarged during regeneration (data not shown).

As shown in Fig. 1N, ductular reactions were first observed at POD 3 in the TGP group. The ductules might have originated from the presumptive area of portal triads and elongated toward the center of the injury. The length and the number of the ductules gradually increased until POD 7 (Fig. 1O-P). Compared with normal BECs, the cells in the ductules had relatively large cytoplasms and round nuclei, although both were smaller than those in

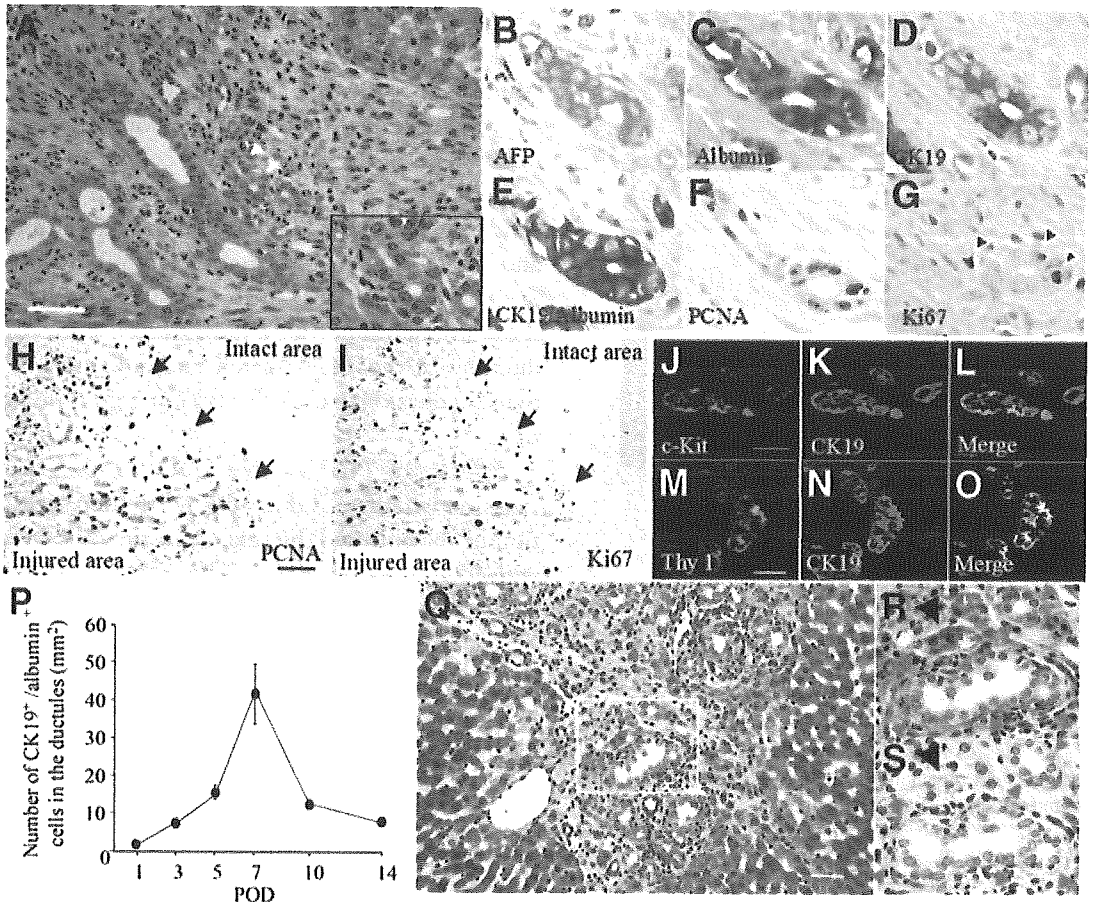

Fig. 2. Characterization of the cells in ductular reactions induced by TGP. Serial sections of the liver tissues were prepared and immunohistochemistry was carried out at POD7. HE staining (A): inset shows the enlargement of the location indicated by white arrowheads. Scale bar, 100 μm. Immunohistochemistry for AFP (B), albumin(C), CK19 (D), PCNA (F, H), and Ki67 (G, I). (E) Double staining of CK19 and albumin. Arrowheads in F and G show Ki67$^+$ nuclei. Immunohistochemistry for PCNA (H) and Ki67 (I) shows that relatively few adjacent hepatocytes (intact area) have positive nuclei at POD 7. Arrows in H and I show the boundary between the injured area and intact area. Scale bar, 100 μm. Fluorescent double immunohistochemistry for c-Kit/CK19 (J-L) and Thy1/CK19 (M-O) of the cells in ductular reactions at POD 7. Scale bar, 100 μm. (P) The number of CK19$^+$/albumin$^+$ cells in the ductules in the upper right quadrant area was counted, which included part of the injured areas. Simultaneously, we measured the size of the area (mm^2) by using NIH image software. Based on the above measurements, we calculated cells/mm^2. The peak of the number was observed at POD 7. We used five rats at each time point, and one slide per rat was prepared for the measurement. The results are shown as mean $\pm$ SEM of five rats. PAS-staining of the cells in ductular reactions at POD 9 (Q-S). (R and S) Enlargement of the square shown in Q. The section was pretreated with diastase before PAS-staining (S). Pinkish granules are observed in the cytoplasm of hepatocyte-like cells around ductules (R, black arrowhead), and basement membrane (positive lines) is surrounding the ductules (red arrows). The pinkish granules in hepatocyte-like cells disappeared after diastase treatment (S, black arrowhead), whereas the linear staining remained around the ductules (S, red arrows). Scale bar, 100 μm. TGF, thermoreversible gelation polymer; POD, postoperative day; FG, fibrin glue; HE, hematoxylin-eosin; AFP, alpha-fetoprotein; PCNA, proliferating cell nuclear antigen; SEM, scanning electron microscopy; PAS, peroidic acid-Schiff.

MHs. The cells in ductules changed their configuration from rectangular to columnar, and hepatocyte-like cells appeared surrounding the ductules (Fig. 1P-Q). At POD 28, the injury lesion was replaced by hepatocytes, and most ductules disappeared. No ductular proliferation was detected in either the control or FG group. Characterization of the cells in ductular reactions was carried out by immunostaining. At POD 7, most cells had CK19, albumin, and AFP (Fig. 2B-E). In addition, 68% and 72% of CK19$^+$ cells in the ductules were c-Kit$^+$ and Thy1$^+$, respectively (Fig. 2J-O). To examine the growth activity of the cells, immunostaining for PCNA and Ki67 was performed. As shown in Fig. 2F-I, many cells in ductular reactions possessed PCNA$^+$ or Ki67$^+$ nuclei, whereas relatively few MHs surrounding the ductular reactions had positive nuclei. The number of CK19$^+$/albumin$^+$ cells in the ductules was counted and the peak was observed at POD 7 (Fig. 2P). The largest numbers of c-Kit$^+$, Thy1$^+$, AFP$^+$, PCNA$^+$ and Ki67$^+$ cells were also observed at POD 7 (data not shown).

As shown in Fig. 2Q-R, hepatocyte-like cells surrounding the ductules appeared at approximately POD 9. To

tapraid5/zhe-hepa/zhe-hepa/zhe00506/zhe1258d06g | heckt | S=7 | 3/6/06 | 15:31 | Art: 05-1402

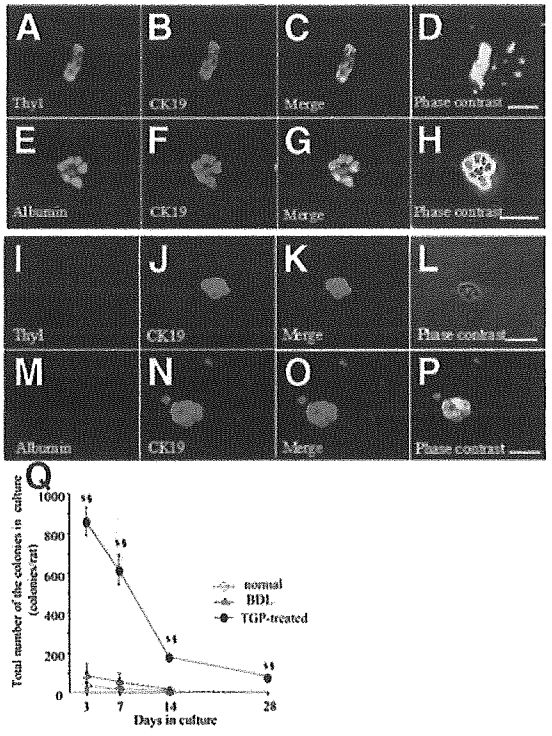

Fig. 3. Characterization of isolation and culture of the ductular cells from a TGP-treated rat liver. Double immunostaining of the cells for Thy1/CK19 (A-C and I-K) and albumin/CK19 (E-G and M-O) was conducted. (D, H, L, and P) Phase-contrast photos of the corresponding cells. Approximately 72% of the isolated cells were Thy1$^+$. CK19$^+$ cells from a normal rat liver were Thy1$^-$ (I) and albumin$^-$ (M). Scale bars, 100 μm. (Q) Total number of colonies per rat. The cells were isolated from normal rats (normal), rats with BDL, and rats treated with TGP (TGP-treated). The ordinate shows the total number of colonies per rat. The points show mean ± SEM of five independent experiments using five rats. TGP versus normal[$] and BDL[§], $P < .05$. TGF, thermoreversible gelation polymer; BDL, bile duct ligated.

examine whether the cells were hepatocytes, PAS staining was performed (Fig. 2R-S). Reddish granules in cytoplasm (Fig. 2R) were observed, and the materials were digested by diastase (Fig. 2S). Conversely, basement membrane surrounding the ductules was not digested. The results proved that the hepatocyte-like cells possessed glycogen in their cytoplasm and were hepatocytes.

Isolation and Culture of Cells in TGP-Induced Ductules. Cells in ductules were isolated from the TGP-treated rat livers and formed small aggregates. To characterize the cells, immunocytochemistry for CK19 and Thy1 was conducted. We found that 89% and 84% of the attached cells were CK19$^+$ and Thy1$^+$, respectively (Fig. 3A-D). Moreover, most CK19$^+$ cells expressed both albumin (Fig. 3E-H) and c-Kit (data not shown). When the same manipulation was performed for rats of the control and FG groups, although few cells were isolated, all cells died in early culture. Therefore, we used BECs from normal and BDL rats as controls. Although all CK19$^+$ BECs isolated from normal and BDL rats survived more than 2 weeks, they did not express Thy1 or albumin (Fig. 3I-P). After plating, the cells from the TGP-treated rats started to grow from day 3 and formed colonies. Colonies sometimes fused and formed a large colony. The number of colonies decreased with time in culture but was significantly higher in the TGP-treated than in both the normal and BDL rats. As shown in Fig. 3Q, the number of ductules from a TGP-treated rat was clearly larger than those from both normal and BDL rats. The cells from the ductules of the TGP-treated rat could survive for more than 60 days. Hepatic cells did not contaminate this culture.

Effects of TGP on the Cells From Ductules. To examine whether TGP could induce hepatic differentiation of the cultured ductular cells, the cells were overlaid with TGP gel from day 7. The cells extensively proliferated, and the colonies became large (Fig. 4D). To exclude the possibility that any gel overlay could induce the differentiation, collagen gel was used as a control. The number of the surviving colonies in all cultures from the 3 groups rapidly decreased with time in culture (Fig. 4E). However, after TGP overlay, the degree of the decrease was suppressed. The slight decrease in the number of colonies in TGP was due to the fusion of neighboring colonies and, therefore, each colony became a large one. Approximately 20 colonies/dish survived in TGP and continued proliferating with time in culture (Fig. 4F). More than 1 month later, cells with large cytoplasm appeared around the periphery of some colonies (Figs. 4G-H). The cells expressed not only albumin but also C/EBPα, which is expressed in differentiated hepatocytes (Fig. 4I). As shown in Fig. 4J, translucent belts were sometimes observed between large cells. These cells expressed albumin (Fig. 4L), and MRP2 was immunocytochemically stained along the structure (Fig. 4K). Therefore, the structures might have been bile canaliculi (BC). Most colonies in NT and CG disappeared by day 42.

To observe the cultured cell ultrastructures, perpendicular sections were prepared using the semithin sections of the samples for TEM. As shown in Fig. 5A, a one- or two-cell layer of columnar cells was arranged on connective tissues, and the cells were larger than 10 × 10 μm, and thus perhaps larger than BEC and smaller than MH. Transversal sections also showed that the colonies consisted of relatively large cells (Fig. 5B). Although the existence of peroxisomes was not proved, the cells possessed many organella such as mitochondria and rough endoplasmic reticulum. In addition, BC-like structures with many microvilli were observed between the cells (Fig. 5C).

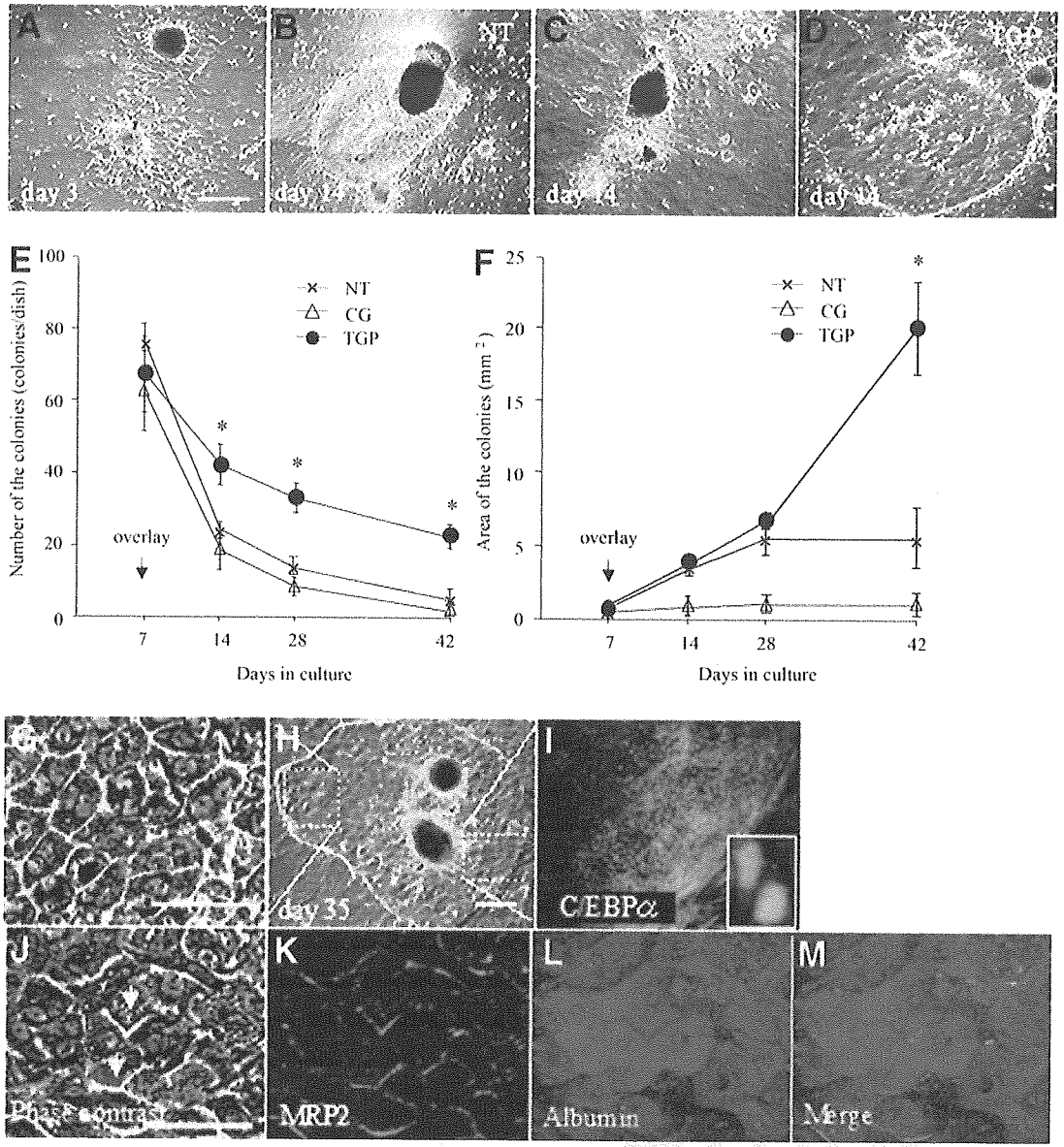

Fig. 4. Culture of the cells isolated from a rat liver treated with TGP. The isolated cells were plated on dishes. The cells initially formed small aggregates and expanded to form colonies with time in culture. Seven days after plating, the cultures were randomly assigned into three groups: Cells were overlaid with nothing (NT), 1 mL collagen gel (CG), and 1 mL TGP gel (TGP). The cells proliferated to form colonies (A), and the colonies continued expanding (B). The cells under CG marginally grew from aggregates (C). The cells under TGP showed rapid expansion to form large colonies (D). The number (E) and the size (F) of the colonies in the cultures were measured. Bars show mean ± SEM of five independent experiments. The number of the colonies at day 3 in each group (NT, CG, and TGP) was 170.8 ± 5.3, 161.6 ± 10.4, and 151.6 ± 7.3, respectively. The area of the colonies at day 3 in each group (NT, CG, and TGP) was 0.26 ± 0.06, 0.21 ± 0.03, and 0.23 ± 0.04 mm^2, respectively. TGP versus *both groups, $P < .05$. Characterization of the cells overlaid with TGP at day 35 (G-M). (G) Enlargement of the location in H indicated by the dotted rectangle. Cells with relatively large cytoplasm are mainly observed in peripheral portions of expanding colonies. Many cells have two nuclei. Scale bar in G, 100 μm. Scale bar in H, 1 mm. Fluorescent immunocytochemistry for C/EBPα (I), MRP2 (K), and albumin (L) was conducted in the cells overlaid with TGP. (I) Enlargement of the portion shown in H indicated by the dotted rectangle. Inset shows a high magnification of the positive nuclei. A phase-contrast photograph of the colony shows that relatively large cells have translucent belts (arrows) between the cells (J). Scale bar, 100 μm. (J and K-M) Phase-contrast micrograph and double immunostaining for MRP2 and albumin of the same cells, respectively. The cells with large cytoplasm are positive for albumin and form translucent belts between the cells. MRP2 is expressed along the belt-like structures. TGF, thermoreversible gelation polymer.

As shown in Table 2, reverse transcription polymerase chain reaction indicated that the isolated cells expressed albumin, transferrin, HNF3α, HNF4, CYP1A1 (hepatic markers), CX43, CK19, CK18 (cholangiocyte markers), AFP, c-Kit, Thy1, and Musashi-1 (immature cell markers).[11] The cells in NT lost the immature cell markers at day 35, and marker genes of differentiated hepatocytes such as TAT, C/EBPα, and CYP2E1 were not detected.

However, when the cultured cells were overlaid with TGP, TAT, C/EBPα, and CYP2E1 genes were expressed at day 35.

Discussion

In rodents and humans, a relationship exists between liver growth and body mass. In resections involving the removal of 40% to 70% of the rodent liver, a linear relationship is seen between the amount of removed tissue and the extent of hepatocyte proliferation. However, the removal of up to 30% of the liver fails to cause a synchronized wave of hepatocyte proliferation after the operation, although the liver eventually regains its mass.[12] In human liver surgery, enucleation of hepatic tumors is performed, and accidental liver injury sometimes occurs. However, the mechanism of the regeneration of a partial defect in the liver is not well understood. Recently, we realized that, when TGP was used as a filler in the partially penetrated liver, we could not find any trace of the injury within 1 month. In the process of hepatic regeneration with TGP, ductular reactions initially appeared at the margins of the area filled with TGP, and the number of inflammatory cells was not large. In addition, although many cells in the ductules showed positive staining of cell cycle–related proteins, proliferation of intact hepatocytes surrounding the injury lesion was relatively few, and the size of the lobules proximal to the lesion did not change after the treatment. This phenomenon was observed only when TGP was used as the filler in the partial defect. When the focal lesion remained untreated (control), exudates immediately filled the space accompanying many inflammatory cells and were then gradually replaced with granulomatous tissue. Even after 1 month, the lesion showed scar formation, and the scar remained for a long time. When FG was used as the filler, a large area of fibrosis in the lesion remained in all rats. Therefore, we considered that the cells in ductular reactions might play an important role in the regeneration of the TGP-treated liver.

The emergence of atypical ductular cells (so-called "ductular reactions") has been reported in some experimental conditions of rodents[13,14] and human liver diseases. For the cellular origin of the ductular reactions, oval cells,[3-5] ductular metaplasia (transdifferentiation from hepatocytes into ductular cells),[13,15] and ductular hepatocytes[3,6,16] have been suggested; however, this is still controversial. In the current experiment, the cells in ductular structures induced by TGP possessed many hepatic proteins such as albumin, transferrin, CYP1A1, HNF3α, and

Table 2. Characterization of the Cells in Ductular Reactions Induced by TGP and the Cultured Cells

Marker Genes	BECs	Cultured Cells (NT)	Isolated Cells	Cultured Cells (TGP)	MHs
Progenitor cells					
Musashi-1	−	−	+	−	−
Oval-cell related					
c-Kit	−	−	+	−	−
Thy1	−	−	+	−	−
AFP	−	−	+	−	−
Hepatocytes					
Albumin	−	+	+	+	+
Transferrin	−	+	+	+	+
TAT	−	−	−	+	+
CYP2E1	−	−	−	+	+
CYP3A1	−	−	−	−	+
Cholangiocytes					
CX43	+	+	+	+	−
CK19	+	+	+	+	−
CK18	+	+	+	+	+
Transcription factors					
HNF3α	−	+	+	+	+
HNF4	−	+	+	+	+
C/EBP α	−	−	−	+	+
HNF6	+	+	+	+	+

NOTE. Gene expression of cell lineage markers was analyzed by semi-quantitative RT-PCR. Total RNA was isolated from BECs (normal rat), the isolated cells in ductular reactions induced by TGP, the cultured cells without overlay (NT) and with TGP (TGP), and MHs (normal rat). Three separate experiments were performed, and the results were reproducible.

−, not detectable; +, detectable.

Abbreviations: BEC, bile epithelial cell; TGP, thermoreversible geiation polymer; NT, no treatment; MH, mature hepatocyte.

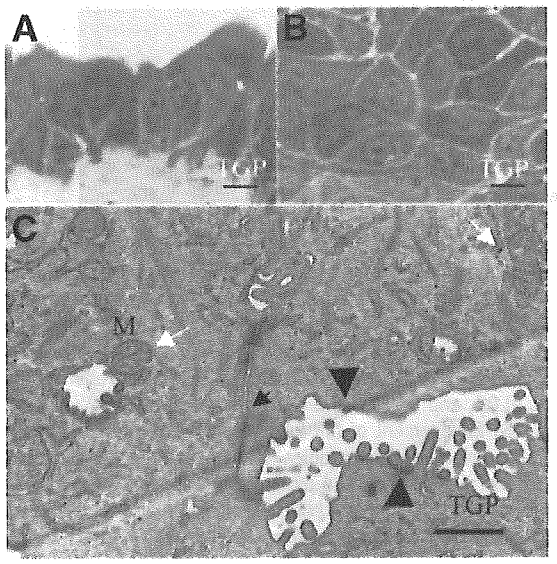

Fig. 5. Perpendicular (A) and horizontal sections (B) of the cultured cells covered with TGP at day 35 (toluidine-blue staining). Hepatocyte-like cells are seen. The size of the cells is between BEC and MH. Scale bars, 10 μm. Ultrastructure of the hepatocyte-like cells at day 35 (C). BC with many microvilli (arrowhead) is shown, and the cytoplasm is rich in organelles such as mitochondria (white arrows) and rough endoplasmic reticulum. A tight junction (an arrow) is observed. Scale bar, 1 μm. TGF, thermoreversible gelation polymer; BEC, bile epithelial cell; MH, mature hepatocyte.

COLOR

HNF4, which were expressed from the initial day of their appearance, although proteins expressed in cholangiocytes and immature hepatocytes were also co-expressed. The features of the cells were initially very similar to terminal BECs. However, the cells gradually became larger after the injury, and the morphological appearance became similar to that of hepatocytes. The morphological alteration of typical cells was observed in the tips of tubular structures at approximately POD 9. The cellular size was intermediate between typical BECs and MHs. In addition, the hepatocyte-like cells increased in the area where the morphological changes of the cells were observed, such as the area surrounding the ductules. The hepatocyte-like cells could produce glycogen in their cytoplasm, and PAS-positive basement membrane around the cells also disappeared. Conversely, they lost the expression of the marker proteins of BECs and immature cells such as CK19, c-Kit, Thy1, and AFP. The cells with hepatobiliary characteristics seemed to differentiate into MHs. With the reduction of the injured area, hepatocyte-like cells rapidly increased, and most of the injured area was occupied by those cells. These results suggest that the cells induced are quite similar to the ductular hepatocytes that were previously reported. The cells have sometimes been observed after massive (or submassive) hepatic necrosis in rats [3,6,16] and in humans.[17-19] Ductular hepatocytes are considered to be an intermediate form between BECs and MHs, resembling ductal plate cells in the developing human liver. They are located at the periphery of the portal tract, proliferate, and express cholangiocyte and hepatocyte markers. However, it has never clearly been shown that ductular hepatocytes can differentiate into and replace ductules with hepatocytes. Fujita et al.[19] demonstrated by sequential liver biopsies over a period of 14 months that a patient who received an auxiliary partial orthotopic liver transplant after suffering massive necrosis had complete regeneration of natural liver.[19] Therefore, we tried to isolate and culture the intermediate cells from ductular reactions induced by TGP. In addition, we examined whether the cells could differentiate into MHs. In this study, isolated cells co-expressing hepatobiliary cell markers could be purified and cultured for a prolonged period. Although many cell aggregates detached from the dish, some survived and expanded after TGP treatment. The overlay of TGP may prevent detachment and stimulate the expansion of the cultured cells. Histological examinations of the TGP-treated rat livers showed that only the BECs close to TGP could extend processes and differentiate into hepatocytes. The ductules far from TGP never showed ductular reactions. In the current experiment, we isolated the cells in ductules from enucleated liver specimens, which included a large area of the margin (10 mm diameter). The margin may have included non-activated BECs, which TGP might not strongly influence. Such non-activated BECs seemed to decrease. The overlay of TGP may stimulate the selective expansion of the cells influenced by TGP.

Oval cells, which are hepatic progenitor cells, are related to terminal biliary ductules and the so-called canals of Hering.[5,20] They are small cells that have an oval-shaped nucleus and scant cytoplasm containing few organelles.[20,21] The oval cells forming ductular structures are usually surrounded by a continuous basement membrane like BECs. Furthermore, they express phenotypic markers of both immature hepatocytes (AFP) and cholangiocytes (CK7, 8, 18, 19, OV6, GGT).[3-5,20,21] In addition, oval cells are known to express hematopoietic stem cell markers such as c-Kit, Thy-1, and CD34.[4,5] In the current experiment, cells in ductular reactions induced by TGP had a round nucleus and relatively large cytoplasm compared with that of oval cells. Although the cells in the ductules immunohistochemically showed expression patterns of AFP, c-Kit, Thy1, and CK19 similar to those of oval cells, they also expressed hepatic markers such as albumin, transferrin, CYP1A1, and HNF4. These genes were not expressed in the oval cells. In addition, oval cells usually appear when hepatic regeneration is impeded by hepatic toxins or the liver is severely damaged. In this study, only a small part of the liver was injured in normal adult rats, and most hepatocytes were intact, as no toxin was systemically administered. These results clearly suggest that the cells induced by TGP are different from oval cells.

Metaplasia of neighboring hepatocytes (ductular metaplasia) into BECs may occur as a result of TGP treatment. In the current experiment, the existence of ductular reactions in the lesion might have been coincident with the suggestive locations of the portal area, which may have existed before the injury. In addition, before the appearance of the ductular reactions at POD 3, although many dead and injured hepatocytes were observed in the area adjacent to TGP, neither a single nor clustered $CK19^+$-cells were randomly detected in those areas. Conversely, at the time of the initial appearance of the cells in ductular reactions, the size and the features of the nuclei were similar to those of BECs.

Thus, TGP itself may have an effect on certain cells to induce differentiation. Recently, it was reported that TGP might have an effect on the renal differentiation of human bone marrow mesenchymal stem cells.[22] Although there is no direct evidence that TGP can play a key role in stem cell differentiation, TGP treatment may directly or indirectly switch on the signal for hepatic differentiation of stem cells in terminal bile ducts or the canal of

tapraid5/zhe-hepa/zhe-hepa/zhe00506/zhe1258d06g | heckt | S=7 | 3/6/06 | 15:31 | Art: 05-1402

Hering. Thus, further investigation is necessary to clarify the molecular mechanism of hepatic differentiation by TGP.

Acknowledgment: We are grateful to Dr. Atsushi Miyajima (Tokyo University, Tokyo, Japan) and Drs. Yuichi Mori, Hiroshi Yoshioka, and Hideo Sakamaki (Waseda University, Tokyo, Japan) for the generous gifts of the rabbit anti-CK19 antibody and TGP, respectively. We also thank Dr. Yoichi Mochizuki for assistance with TEM and Minako Kuwano, Shigeko Ohnuma, Akiko Hosoyama, Erika Takada, Hiroshi Kohara, Izuru Yokomi, and Tsuneo Igarashi for their technical assistance. We also thank Kim Barrymore for help with the manuscript.

References

1. Nagaya M, Kubota S, Suzuki N, Tadokoro M, Akashi K. Evaluation of thermoreversible gelation polymer for regeneration of focal liver injury. Eur Surg Res 2004;36:95-103.
2. Yoshioka H, Mikami M, Mori Y, Tsuchida E: A synthetic hydrogel with thermoreversible gelation: preparation and rheological properties. J Macromol Sci 1994;A31:113-120
3. Sell S. The role of progenitor cells in repair of liver injury and in liver transplantation. Wound Repair Regen 2001;9:467-482.
4. Fausto N. Liver regeneration and repair: hepatocytes, progenitor cells, and stem cells. HEPATOLOGY 2004;39:1477-1487.
5. Alison MR, Vig P, Russo F, Bigger BW, Amofah E, Themis M, et al. Hepatic stem cells: from inside and outside the liver? Cell Prolif 2004;37:1-21.
6. Sirica AE, Williams TW. Appearance of ductular hepatocytes in rat liver after bile duct ligation and subsequent zone 3 necrosis by carbon tetrachloride. Am J Pathol 1992;140:129-136.
7. Wagers AJ, Sherwood RI, Christensen JL, Weissman IL. Little evidence for developmental plasticity of adult hematopoietic stem cells. Science 2002; 297:2256-2259.
8. Tsanadis G, Kotoulas O, Lollis D. Hepatocyte-like cells in the pancreatic islets: study of the human foetal pancreas and experimental models. Histol Histopathol 1995;10:1-10.
9. Mitaka T, Sato F, Mizuguchi T, Yokono T, Mochizuki Y. Reconstruction of hepatic organoid by rat small hepatocytes and hepatic nonparenchymal cells. HEPATOLOGY 1999;29:111-125.
10. Yang L, Li S, Hatch H, Ahrens K, Cornelius JG, Petersen BE, et al. In vitro trans-differentiation of adult hepatic stem cells into pancreatic endocrine hormone-producing cells. Proc Natl Acad Sci U S A 2002; 99:8078-8083.
11. Miura K, Nagai H, Ueno Y, Goto T, Mikami K, Nakane K, et al. Epimorphin is involved in differentiation of rat hepatic stem-like cells through cell-cell contact. Biochem Biophys Res Commun 2003;311:415-423.
12. Bucher NL. Regeneration of mammalian liver. Int Rev Cytol 1963;15: 245-300.
13. Desmet V, Roskams T, Van Eyken P: Ductular reaction in the liver. Pathol Res Pract 1995;191:513-524.
14. Popper H. The relation of mesenchymal cell products to hepatic epithelial system. In: Popper H, Schaffner F, eds. Progress in Liver Diseases. Philadelphia: W.B. Saunders, 1990:27-38.
15. Michalopoulos GK, Barua L, Bowen WC. Transdifferentiation of rat hepatocytes into biliary cells after bile duct ligation and toxic biliary injury. HEPATOLOGY 2005;41:535-544.
16. Sirica AE. Ductular hepatocytes. Histol Histopathol 1995;10:433-456.
17. Roskams T, De Vos R, Van Eyken P, Myazaki H, Van Damme B, Desmet V. Hepatic OV-6 expression in human liver disease and rat experiments: evidence for hepatic progenitor cells in man. J Hepatol 1998;29:455-463.
18. Haque S, Haruna Y, Saito K, Nalesnik MA, Atillasoy E, Thung SN, et al. Identification of bipotential progenitor cells in human liver regeneration. Lab Invest 1996;75:699-705.
19. Fujita M, Furukawa H, Hattori M, Todo S, Ishida Y, Nagashima K. Sequential observation of liver cell regeneration after massive hepatic necrosis in auxiliary partial orthotopic liver transplantation. Mod Pathol 2000;13:152-157.
20. Paku S, Nagy P, Kopper L, Thorgeirsson SS. 2-Acetylaminofluorene dose-dependent differentiation of rat oval cells into hepatocytes: confocal and electron microscopic studies. HEPATOLOGY 2004;39:1353-1361.
21. Hixson DC, Faris RA, Thompson NL. An antigenic portrait of the liver during carcinogenesis. Pathobiology 1990;58:65-77.
22. Hishikawa K, Miura S, Marumo T, Yoshioka H, Mori Y, Takato T, et al. Gene expression profile of human mesenchymal stem cells during osteogenesis in three-dimensional thermoreversible gelation polymer. Biochem Biophys Res Commun 2004;317:1103-1107.